SYNTHESIS OF POTASSIUM FERRITE BY PRECURSOR AND COMBUSTION METHODS
A comparative study

B. S. Randhawa[1][*], *H. S. Dosanjh*[1] *and N. Kumar*[2]

[1]Department of Chemistry, Guru Nanak Dev University, Amritsar, Punjab, India
[2]Solid State Physics Laboratory (DRDO), Timarpur, New-Delhi, India

The thermolysis of potassium hexa(carboxylato)ferrate(III) precursors, $K_3[Fe(L)_6] \cdot xH_2O$ (*L*=formate, acetate, propionate, butyrate), has been carried out in flowing air atmosphere from ambient temperature to 900°C. Various physico-chemical techniques i.e. TG, DTG, DTA, XRD, IR, Mössbauer spectroscopy etc. have been employed to characterize the intermediates and end products. After dehydration, the anhydrous complexes undergo exothermic decomposition to yield various intermediates i.e. potassium carbonate/acetate/propionate/butyrate and α-Fe_2O_3. A subsequent decomposition of these intermediates leads to the formation of potassium ferrite ($KFeO_2$) above 700°C. The same ferrite has also been prepared by the combustion method at a comparatively lower temperature (600°C) and in less time than that of conventional ceramic method.

Keywords: *chemical synthesis, Mössbauer spectroscopy, oxides, thermal analysis (TG-DTG-DTA)*

Introduction

Mixed metallic oxides are designated as an important class of compounds and among them ferrites are most prominent by virtue of their high electrical resistivity, thermodynamic stability, electro-catalytic activity and resistance to corrosion. Ferrites are regarded as better magnetic materials than pure metals because of their high resistivity, lower cost, easier manufacture and superior magnetization properties. Thermal decomposition studies serve as the most useful tool to get insight into the mechanism of solid-state decomposition of ferricarboxylates. Thermal decomposition of metal ferricarboxylate precursors has been extensively exploited in the past two decades to prepare oxide/ferrite nanoparticles with controlled stoichiometry, high homogeneity and reduced particle size [1–3]. Alkali metal ferrites have attracted a considerable attention owing to their potential application in high capacity batteries [4], waste–water cleaning [5], low magnetization ferrofluids [6], intercalation electrodes in rechargeable batteries [7] and as strong oxidizing agents [8]. The same ferrites have also been synthesized by employing another important route i.e. solution phase combustion method which involves the formation of stoichiometrically pure and single-phase nanoparticles [9, 10]. On the other hand the conventional ceramic method, which is the most common technique for bulk preparation of ferrites, involves high temperature sintering of reactant oxides coupled with frequent milling. Since high sintering temperature results in particle coarsening and aggregation, nanoparticle ferrites cannot be obtained by this method [11, 12].

In the present investigation we report the synthesis of $KFeO_2$ from the thermal decomposition of potassium ferricarboxylate precursors ($K_3[Fe(L)_6] \cdot xH_2O$) and by solution phase combustion method.

Experimental

Precursor method

Potassium ferricarboxylate precursors, $K_3[Fe(L)_6] \cdot xH_2O$ (*L*=formate, acetate, propionate, butyrate) were prepared by mixing stoichiometric quantities of aqueous solutions of ferric nitrate, respective potassium carboxylate and carboxylic acid. The reaction mixture was stirred vigorously at 60°C till a clear solution was obtained. It was concentrated on water bath until a brown colored product was formed. The product was filtered, washed with cold water, air dried and stored in vacuum desiccator. The identity of the complexes (precursors) was established by elemental analysis (Table 1). The percentage of iron was determined spectrophotometrically using 1,10-phenanthroline [13]. Potassium content in each precursor was determined flame-photometrically.
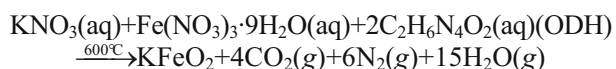
* Author for correspondence: balwinderrandhawa@yahoo.co.in

Table 1 Composition of the potassium ferricarboxylate precursors

Complex		C/%	H/%	Fe/%	K/%
$K_3[Fe(HCOO)_6] \cdot 3H_2O$	Obsd.	14.44	2.36	11.25	23.48
	Calc.	14.48	2.41	11.27	23.54
$K_3[Fe(CH_3COO)_6] \cdot 3H_2O$	Obsd.	24.74	4.09	9.60	20.11
	Calc.	24.78	4.13	9.64	20.14
$K_3[Fe(CH_3CH_2COO)_6] \cdot 4H_2O$	Obsd.	31.57	5.51	8.17	17.12
	Calc.	31.62	5.56	8.20	17.13
$K_3[Fe(CH_3CH_2CH_2COO)_6] \cdot 7H_2O$	Obsd.	34.98	6.76	6.78	14.22
	Calc.	35.08	6.82	6.82	14.25

Solution phase combustion method

Oxalyl dihydrazide, (ODH), required for the preparation of ferrites by combustion synthesis, was prepared by the method reported elsewhere [10]. For the preparation of ferrites, the stoichiometric quantities of aqueous solutions of KNO_3, $Fe(NO_3)_3 \cdot 9H_2O$ and oxalyl dihydrazide (ODH) were mixed in a pyrex dish. The reaction mixture was combusted in a muffle furnace maintained at 600°C. The entire combustion process was over in 30 min to yield ferrite by the following redox reaction:

$$KNO_3(aq) + Fe(NO_3)_3 \cdot 9H_2O(aq) + 2C_2H_6N_4O_2(aq)(ODH)$$
$$\xrightarrow{600°C} KFeO_2 + 4CO_2(g) + 6N_2(g) + 15H_2O(g)$$

Infrared (IR) spectra of potassium ferricarboxylate precursors and their thermolysis products were recorded on Pye-Unicam SP3-300 IR spectrometer in the range 4000–400 cm^{-1} using KBr matrix. Simultaneous TG-DTG-DTA curves were recorded on a Pyris Diamond Model (Perkin Elmer) at a heating rate of 5°C min^{-1}. XRD powder patterns were recorded at IIT, New Delhi using nickel filtered CuK_α radiation. ^{57}Fe Mössbauer spectra were recorded on Wissel (Germany) Mössbauer spectrometer. A ^{57}Co(Rh) γ-ray source was employed and the velocity scale was calibrated relative to ^{57}Fe in Rh matrix. Mössbauer spectral analysis software WinNormos for Igor Pro has been used for the quantitative evaluation of the spectral parameters. Isomer shift values are reported with respect to pure iron absorber.

For the identification of intermediates and products, the precursors were also calcined isothermally in nickel crucibles. The variation in temperature was kept ±5°C during isothermal calcinations.

Results and discussion

Characterization of potassium ferrite prepared by precursor method

IR spectrum of potassium hexa(formato)ferrate(III) trihydrate precursor shows a broad band centered at about 3265 cm^{-1} due to ν_{O-H} of lattice water and a distinct shoulder at 2875 cm^{-1} due to ν_{C-H} of the formate group. Intense bands in the ranges 1620–1670 and 1360–1415 cm^{-1} are attributed to $\nu_{asy(C=O)}$ and $\nu_{sym(C=O)}$ of the coordinated formate groups [14], respectively. A small but distinct band at 575 cm^{-1} due to ν_{Fe-O} suggests the presence of Fe–O (carboxylate) bonding [15]. The other precursors i.e. potassium hexa(acetato)ferrate(III) trihydrate, potassium hexa(propionato)ferrate(III) tetrahydrate and potassium hexa(butyrato)ferrate(III) heptahydrate display almost similar IR spectra.

Mössbauer spectra of the potassium ferricarboxylate precursors exhibit a doublet (Fig. 1) with isomer shift (δ) and quadrupole splitting (Δ) values in the ranges 0.28–0.31±0.005 and 0.45–0.49±0.007 mm s^{-1}, respectively. These parameters correspond to those reported for high spin ferric ions in octahedral coordination [16]. The coordination number of six for iron is satisfied by six formate ligands, which bind to iron through oxygen atoms of the carboxylate groups. The outer cation (K^+) and water molecules seem to be responsible for linking to-
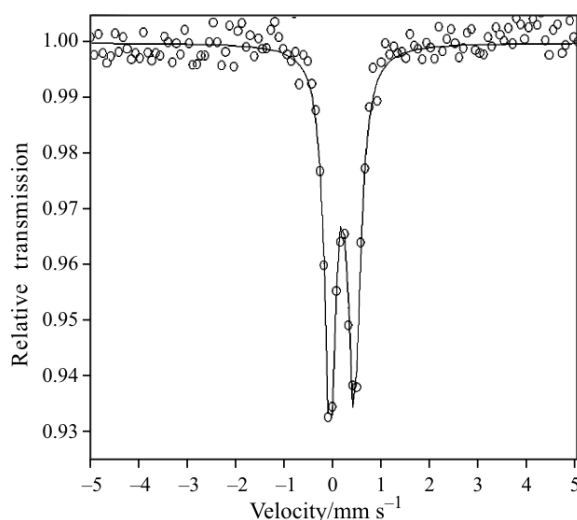

Fig. 1 Mössbauer spectrum of potassium hexa(formato)ferrate(III) trihydrate

gether the complex ion, $[Fe(L)_6]^{3-}$. The high spin nature of iron(III) in these precursors has also been confirmed by their magnetic susceptibility values that lie in the range 5.82–5.92 B.M.

Thermal decomposition studies

The compoundwise discussion on the thermal decomposition of various potassium hexa(carboxylato)ferrate(III) precursors follows:

Potassium hexa(formato)ferrate(III) trihydrate, $K_3[Fe(HCOO)_6]\cdot 3H_2O$

Figure 2 shows the simultaneous TG-DTG-DTA curves of potassium hexa(formato)ferrate(III) trihydrate in flowing air atmosphere at a heating rate of 5°C min^{-1}. The complex undergoes dehydration till a mass loss of 10.5% is reached at 190°C (calc. loss=10.8%). The corresponding broad DTA (endotherm) and DTG peaks are centered at about 125 and 120°C, respectively. The anhydrous complex undergoes exothermic decomposition to yield potassium carbonate and Fe_2O_3 until a mass loss of 41.5% is reached at 250°C (calc. loss=42.2%). Corresponding to this step, DTA shows an exotherm at 245°C while DTG also displays a respective distinct signal at 245°C. The presence of α-Fe_2O_3 has been confirmed by recording the Mössbauer spectrum (Fig. 3) of the residue obtained by calcining the precursor isothermally at 250°C for 15 min. The shape of the spectrum and Mössbauer parameters resemble to those reported [17, 18] for a cluster of α-Fe_2O_3 particles with an average grain size of 15 nm. The particles with diameters less than 10 nm present in the cluster show a central doublet while for the particles with diameters greater than 10 nm, a hyperfine spectrum develops at the cost of central doublet. As the heating continues, K_2CO_3 decomposes into K_2O followed by a
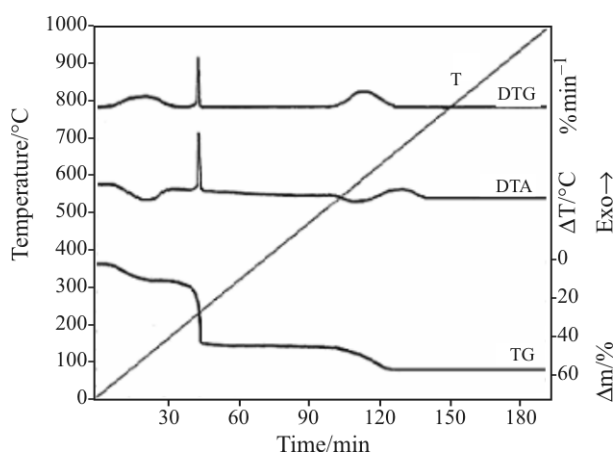
solid-state reaction between K_2O and α-Fe_2O_3 to yield potassium ferrite i.e. $KFeO_2$ as indicated by a mass loss of 55.1% at 670°C (calc. loss=55.5%). Both these thermal changes are reflected by the corresponding endotherm and exotherm with peak maxima at 600 and 675°C, respectively in DTA. DTG also shows respective signal for the endo-decomposition. In order to obtain pure potassium ferrite i.e. $KFeO_2$, the final thermolysis product was washed repeatedly with distilled water to remove unreacted K_2O [19]. The identity of the ferrite has been confirmed by recording Mössbauer spectrum (Fig. 4) of the final residue, which shows a doublet with hyperfine parameters δ=0.22 mm s^{-1} and Δ=0.46 mm s^{-1}. These parameters (Table 2) are in agreement to those reported for Fe^{3+} ions in tetrahedral co-ordination [16, 20]. The presence of quadrupole splitting shows a slight distortion from regular tetrahedral geometry.
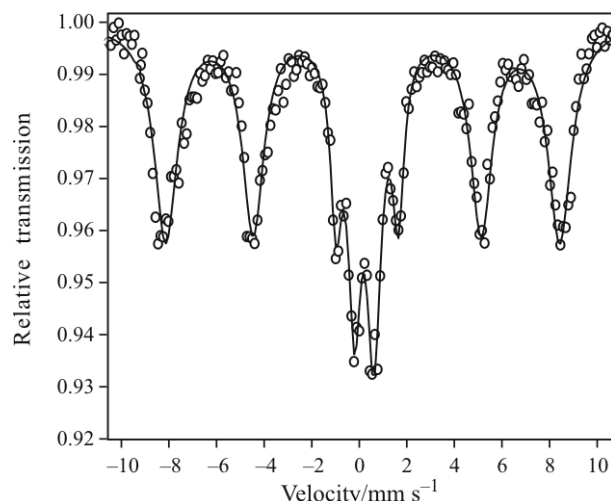

Fig. 3 Mössbauer spectrum of the residue obtained after calcining the parent complex at 260°C for 15 min
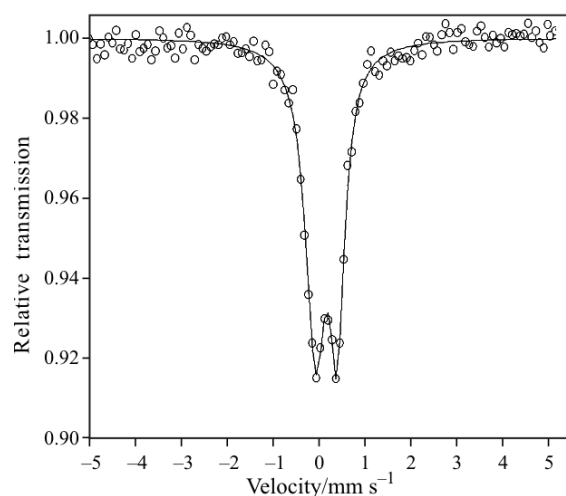

Fig. 2 Simultaneous TG-DTG-DTA curves of potassium hexa(formato)ferrate(III) trihydrate

Fig. 4 Mössbauer spectrum of the final thermolysis product of potassium hexa(formato)ferrate(III) trihydrate

Table 2 Mössbauer parameters for the thermolysis products of $K_3[Fe(L)_6] \cdot xH_2O$ recorded at 25°C

L	Temp. of calcination/°C	$\delta^{\#}/$ mm s^{-1}	$\Delta/$ mm s^{-1}	B(T)	Assignment
HCOO	250	0.34±0.004	–0.18±0.017	51.4±0.048(S)	α-Fe$_2$O$_3$
		0.32±0.011	0.82±0.015	---(CD)	
	720	0.22±0.006	0.46±0.006	---	KFeO$_2$
CH$_3$COO	275	0.33±0.006	–0.18±0.014	51.3±0.055(S)	α-Fe$_2$O$_3$
		0.31±0.013	0.81±0.018	---(CD)	
	800	0.21±0.004	0.47±0.004	---	KFeO$_2$
CH$_3$CH$_2$COO	270	0.35±0.003	–0.17±0.012	51.3±0.057(S)	α-Fe$_2$O$_3$
		0.31±0.016	0.81±0.010	---(CD)	
	790	0.22±0.003	0.46±0.003	---	KFeO$_2$
CH$_3$CH$_2$CH$_2$COO	285	0.34±0.006	–0.19±0.014	51.5±0.052(S)	α-Fe$_2$O$_3$
		0.32±0.013	0.83±0.011	---(CD)	
	760	0.23±0.005	0.48±0.005	---	KFeO$_2$

$^{\#}$w.r.t. pure iron absorber

B=Internal magnetic field in Tesla (*T*), S=Sextet, CD=Central doublet
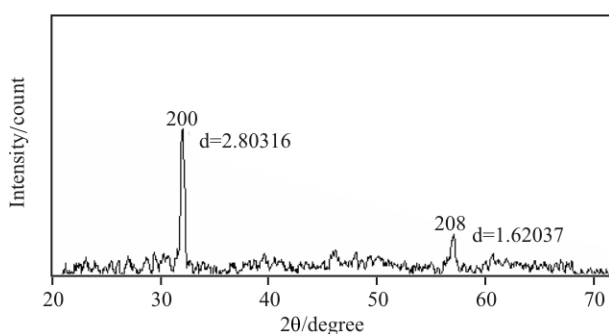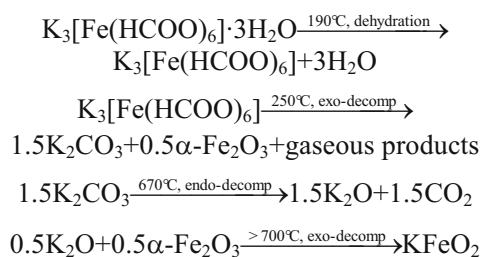

Fig. 5 XRD powder pattern of the final thermolysis product of potassium hexa(formato)ferrate(III) trihydrate

XRD powder pattern (Fig. 5) of the final thermolysis residue also reveals the existence of KFeO$_2$.

Based on the above discussion, the following pathway for the thermal decomposition of potassium hexa(formato)ferrate(III) trihydrate is proposed:

$$K_3[Fe(HCOO)_6] \cdot 3H_2O \xrightarrow{190°C, \text{ dehydration}}$$
$$K_3[Fe(HCOO)_6] + 3H_2O$$

$$K_3[Fe(HCOO)_6] \xrightarrow{250°C, \text{ exo-decomp}}$$
$$1.5K_2CO_3 + 0.5\alpha\text{-Fe}_2O_3 + \text{gaseous products}$$

$$1.5K_2CO_3 \xrightarrow{670°C, \text{ endo-decomp}} 1.5K_2O + 1.5CO_2$$

$$0.5K_2O + 0.5\alpha\text{-Fe}_2O_3 \xrightarrow{>700°C, \text{ exo-decomp}} KFeO_2$$

Potassium hexa(acetato)ferrate(III) trihydrate, $K_3[Fe(CH_3COO)_6] \cdot 3H_2O$

Figure 6 presents the simultaneous TG-DTG-DTA curves of potassium hexa(acetato)ferrate(III) trihydrate at a heating rate of 5°C min^{-1}. Dehydration of the precursor commences at 88 and completes at 163°C as indicated by a mass loss of 9.0% (calc. loss=9.2%). The corresponding broad DTA (endothermic) and DTG peaks are centered at 126 and 124°C, respectively. Anhydrous
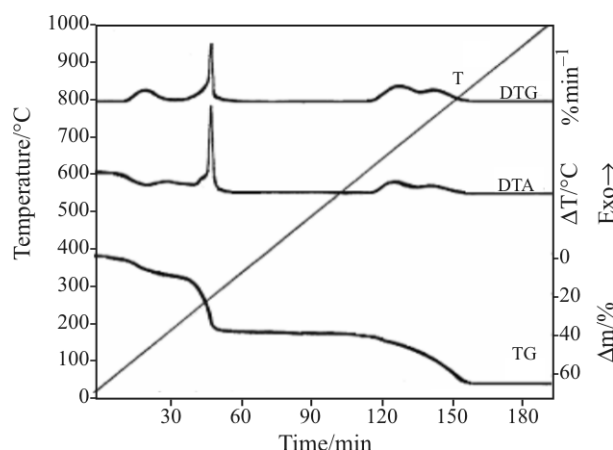

Fig. 6 Simultaneous TG-DTG-DTA curves of potassium hexa(acetato)ferrate(III) trihydrate

potassium ferriacetate then undergoes exothermic decomposition to yield potassium acetate and Fe$_2$O$_3$ till a mass loss of 35.2% is reached at 275°C (calc. loss=35.6%). Corresponding to this step, DTA shows an exotherm at 272°C while the respective DTG peak lies at 270°C. As the heating continues potassium acetate and α-Fe$_2$O$_3$ undergoes decomposition to yield K$_2$O and KFeO$_2$ as indicated by a mass loss of 61.8% at 800°C (calc. loss= 62.0%). This step is accompanied by doublets in DTA (exotherm) and DTG suggesting that two thermal changes are taking place i.e. breakdown of potassium acetate into carbonate followed by its decomposition to oxide/ferrite. In order to obtain pure potassium ferrite i.e. KFeO$_2$ the final thermolysis product was washed with distilled water to remove K$_2$O. The identity of the ferrite as KFeO$_2$ has been revealed by Mössbauer parameters (Table 2) of the final thermolysis product and XRD powder pattern.

Based on the above results, the following mechanism for the thermal decomposition of potassium hexa(acetato)ferrate(III) trihydrate is suggested:
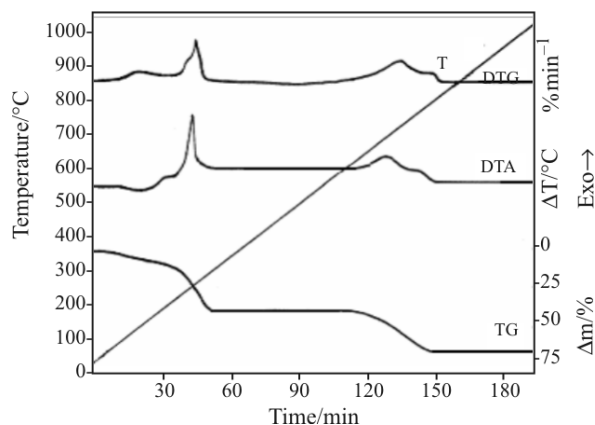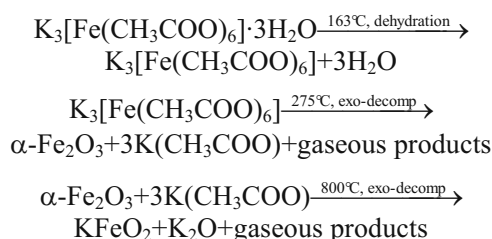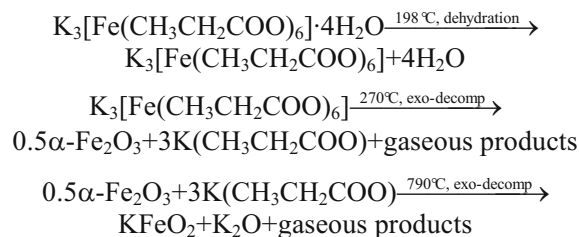
Fig. 7 Simultaneous TG-DTG-DTA curves of potassium hexa(propionato)ferrate(III) tetrahydrate

$$K_3[Fe(CH_3COO)_6]\cdot3H_2O \xrightarrow{\text{163°C, dehydration}} K_3[Fe(CH_3COO)_6]+3H_2O$$

$$K_3[Fe(CH_3COO)_6] \xrightarrow{\text{275°C, exo-decomp}} \alpha\text{-}Fe_2O_3+3K(CH_3COO)+\text{gaseous products}$$

$$\alpha\text{-}Fe_2O_3+3K(CH_3COO) \xrightarrow{\text{800°C, exo-decomp}} KFeO_2+K_2O+\text{gaseous products}$$

Potassium hexa(propionato)ferrate(III) tetrahydrate, $K_3[Fe(CH_3CH_2COO)_6]\cdot4H_2O$

Figure 7 exhibits the simultaneous TG-DTG-DTA curves of potassium hexa(propionato)ferrate(III) tetrahydrate precursor in flowing air atmosphere at a heating rate of 5°C min^{-1}. The precursor undergoes dehydration up to 198°C as indicated by a mass loss of 10.5% (calc. loss=10.5%). DTA shows corresponding broad endotherm centered at 132°C and accompanied by a DTG peak centered at 130°C. The anhydrous precursor undergoes an oxidative decomposition process with a mass loss of 39.0% at 270°C suggesting the formation of Fe_2O_3 and potassium propionate (calc. loss=39.4%). Corresponding to this step, DTG shows a peak at 250°C while DTA exhibits an exotherm centered at 255°C. The existence of Fe_2O_3 has been confirmed by recording Mössbauer parameters (Table 2) of the residue obtained by calcining the precursor isothermally at 270°C for 15 min. As heating continues, potassium propionate and $\alpha\text{-}Fe_2O_3$ get decomposed into $KFeO_2$ and K_2O with a mass loss of 67.5% at 790°C (calc. loss=67.6%). There exist corresponding peaks with shoulders in DTA (exotherm) and DTG suggesting a multi-step decomposition process. The identity of the end product as $KFeO_2$ has been confirmed from its Mössbauer parameters (Table 2) and XRD powder pattern.

Based on the above observations, the following pathway for the aerial thermal decomposition of potassium hexa(propionato)ferrate(III) tetrahydrate precursor is proposed:

$$K_3[Fe(CH_3CH_2COO)_6]\cdot4H_2O \xrightarrow{\text{198°C, dehydration}} K_3[Fe(CH_3CH_2COO)_6]+4H_2O$$

$$K_3[Fe(CH_3CH_2COO)_6] \xrightarrow{\text{270°C, exo-decomp}} 0.5\alpha\text{-}Fe_2O_3+3K(CH_3CH_2COO)+\text{gaseous products}$$

$$0.5\alpha\text{-}Fe_2O_3+3K(CH_3CH_2COO) \xrightarrow{\text{790°C, exo-decomp}} KFeO_2+K_2O+\text{gaseous products}$$

Potassium hexa(butyrato)ferrate(III) heptahydrate, $K_3[Fe(CH_3CH_2CH_2COO)_6]\cdot7H_2O$

The thermal decomposition pattern of potassium hexa(butyrato)ferrate(III) heptahydrate (Fig. 8) has been found to be almost similar to that observed for its propionate counterpart. The identity of the end product as $KFeO_2$ has been revealed by its Mössbauer parameters (Table 2) and XRD powder pattern.

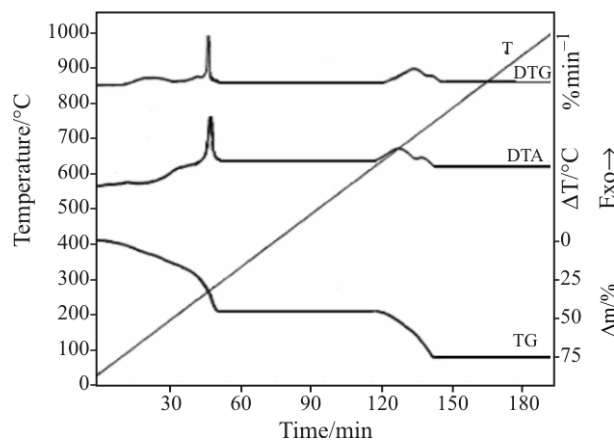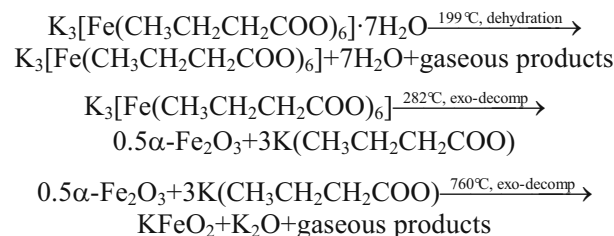The decomposition process proceeds by the following mechanism:

$$K_3[Fe(CH_3CH_2CH_2COO)_6]\cdot7H_2O \xrightarrow{\text{199°C, dehydration}} K_3[Fe(CH_3CH_2CH_2COO)_6]+7H_2O+\text{gaseous products}$$

$$K_3[Fe(CH_3CH_2CH_2COO)_6] \xrightarrow{\text{282°C, exo-decomp}} 0.5\alpha\text{-}Fe_2O_3+3K(CH_3CH_2CH_2COO)$$

$$0.5\alpha\text{-}Fe_2O_3+3K(CH_3CH_2CH_2COO) \xrightarrow{\text{760°C, exo-decomp}} KFeO_2+K_2O+\text{gaseous products}$$

Fig. 8 Simultaneous TG-DTG-DTA curves of potassium hexa(butyrato)ferrate(III) heptahydrate

Characterization of potassium ferrite prepared by combustion (solution-phase) method

The ferrite, $KFeO_2$ obtained from the solution phase combustion of redox mixture (potassium nitrate, ferric nitrate and ODH) has been characterized by XRD powder pattern (Fig. 9) and Mössbauer spectrum (Fig. 10) which exhibits a symmetrical doublet with isomer shift and quadruple splitting values of 0.22 and 0.47 mm s^{-1}, respectively. These parameters correspond to ferric ions in tetrahedral coordination [16, 20].
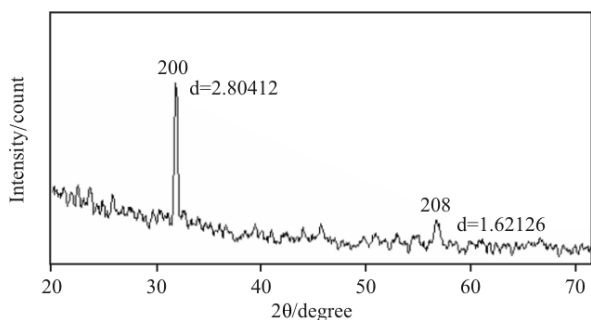
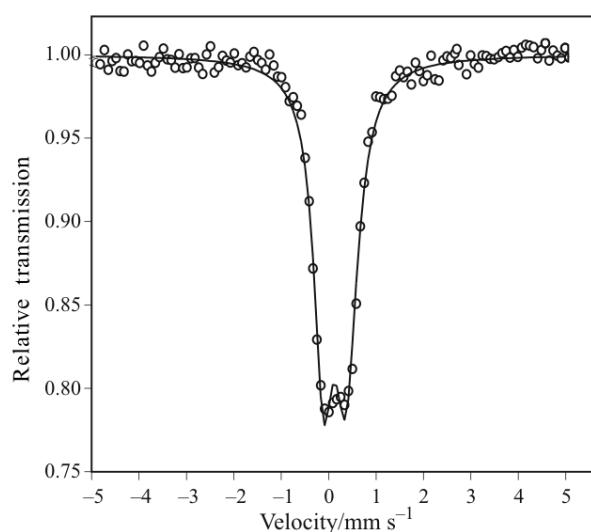Fig. 9 XRD powder pattern of KFeO₂ prepared by combustion method

Fig. 10 Mössbauer spectrum of KFeO₂ prepared by combustion method

Conclusions

Single phase $KFeO_2$ powders have been successfully prepared by precursor as well as combustion methods. The thermal decomposition of potassium ferricarboxylate precursors proceeds without undergoing reduction to iron(II) state. The reduction of Fe(III) to Fe(II) being endothermic process takes up some heat, thus, causing the ferrite formation at higher temperature as has been observed in the thermolysis of alkali metal ferrioxalate precursor [21]. The solution phase combustion method is rapid and undergoes a direct conversion from the molecular mixture of the precursor solution to the final oxide (ferrite) product, avoiding the formation of intermediate phases that require inter-diffusion for complete reaction.

In both these methods, stoichiometrically pure ferrites are obtained at lower temperature and in shorter time. Further no milling of starting materials is required (necessary in ceramic method) that can introduce lattice defects in the ferrite obtained which, in turn, affect its permanent magnetic properties.

References

1 B. S. Randhawa, H. S. Dosanjh and N. Kumar, J. Radioanal. Nucl. Chem., 274 (2007) 581.
2 B. S. Randhawa and K. Gandotra, J. Therm. Anal. Cal., 85 (2006) 417.
3 B. S. Randhawa and M. Kaur, J. Therm. Anal. Cal., 89 (2007) 251.
4 S. Licht, B. Wang and S. Ghosh, Science, 285 (1999) 1039.
5 V. K. Sharma, J. O. Smith and F. J. Millero, Environ. Sci. Technol., 31 (1997) 2486.
6 V. K. Sankaranarayanan, O. Prakash, R. P. Pant and M. Islam, J. Magn. Magn. Mater., 252 (2002) 7.
7 R. B. Goldner, F. O. Arntz, G. Berera, T. E. Haas, G. Wei, K. K. Wong and P. C. Yu, Solid State Ionics, 617 (1992) 53.
8 L. Delaude and P. László, J. Org. Chem., 61 (1996) 6360.
9 K. J. Rao, Perspectives in Solid State Chemistry, Narosa Publication House, New Delhi 1995.
10 B. S. Randhawa, H. S. Dosanjh and M. Kaur, Ind. J. Eng. Mat. Sci., 12 (2005) 151.
11 C. N. R. Rao and J. Gopalkrishanan, New Directions in Solid State Chemistry, Cambridge University Press, UK 1997.
12 M. J. Ruthner, J. Phys., 7 (1997) CI-53.
13 A. I. Vogel, A text book of Quantitative Inorganic Analysis Including Elementary Instrumental Analysis, English Language Book Society and Longman, London 1973.
14 K. Nakamoto, Infrared Spectra of Inorganic and Coordination Compounds, John Wiley Intersci., 2nd Ed., New York 1970.
15 J. R. Ferraro, R. Driver, W. R. Walker and W. Wozniak, Inorg. Chem., 6 (1967) 1586.
16 F. Menil, J. Phys. Chem. Solids, 46 (1985) 763.
17 S. S. Bellad, C. D. Lokhande and C. H. Bhosale, Ind. J. P. Appl. Phys., 35 (1997) 565.
18 W. Kundig, H. Bommel, G. Constabaris and R. H. Lindquist, Phys. Rev., 142 (1966) 327.
19 G. G. Hawley, The Condensed Chemical Dictionary, Eighth Ed., Van Nostrand Reinhold Company, New York 1971.
20 T. Birchall, N. N. Greenwood and A. F. Reid, J. Chem. Soc. A, (1969) 2382.
21 A. S. Brar and B. S. Randhawa, J. Solid State Chem., 58 (1985) 153.